METABOLISM OF 4-HYDROXY TRANS 2- NONENAL (HNE) IN CULTURED PC-12 CELLS

MA Siddiqui, MP Kashyap, VK Khanna, VK Gupta, VK Tripathi, S Srivastva*, AB Pant

Indian Institute of Toxicology Research, Lucknow-India (Council of Scientific & Industrial Research, New Delhi)
*Institute of Molecular Cardiology, University of Louisville, Louisville, KY, USA

***Corresponding Author** :*
Dr. A B Pant
Scientist,
In Vitro *Toxicology Laboratory*
Indian Institute of Toxicology Research
P.O. Box: 80, MG Marg
Lucknow-226001 (UP) India
Voice: +91-522-2627586 Ext.: 321 (Work)
+91-9935044044 (Mobile)
Fax : +91-522-2628227
Email : abpant@rediffmail.com; abpant@yahoo.com
(Date received: 14/07/2008)

Abstract

One of the most reactive aldehyde generated from the lipid peroxidation reactions is α, β-unsaturated aldehyde, 4,hydroxyl trans-2-nonenal (HNE). Due to α, β-unsaturation, HNE is extremely reactive molecule. At low concentrations, HNE is involved in cell signaling whereas higher concentrations of HNE are cytotoxic (1). The biological effects of HNE will be dependent on the metabolism of HNE. The present investigations were carried out to examine the metabolism of HNE in PC-12 cells and to study the cytotoxic effects of HNE as well as the effect of non-toxic concentrations of HNE on neurotransmitter receptors. Our data shows that in PC-12 cells, at low (physiological) concentrations HNE is primarily metabolized by glutathiolation and oxidation, whereas at higher (pathological) concentrations, in addition to glutathiolation and oxidation, a significant fraction of HNE is reduced in PC-12 cells. Moreover, at higher concentrations, HNE also shows the abundance of two hydrophobic peaks, the structural identities of which has yet not been established. Mass spectroscopic analysis also shows that glutathionyl adduct of HNE is present as two forms-GS-HNE and its reduced metabolite GS-DHN. However, unlike the cardiovascular cells, reduction of GS-HNE is not catalyzed by aldose reductase, since inhibition of aldose reductase, did not abolish the reduction of GS-HNE in PC-12 cells. However, similar to other cells, oxidation of HNE in PC-12 cells was significantly inhibited by aldehyde dehydrogenase inhibitor, benomyl, suggesting that aldehyde dehydrogenase-mediated oxidation of HNE is an important route for the elimination of HNE in neuronal cells.

Key Words: PC-12 cells, HNE metabolism, oxidoreductases

Introduction:

Oxidative stress has been implicated in the etiology of several disease processes including atherosclerosis, ischemia-reperfusion, neurological disorders, rheumatic arthritis, diabetes and cancer. Amongst the cerebro-vascular disorders, increasing levels of lipid peroxidation products have been detected in Alzheimer's disease (AD), multiple sclerosis, Parkinson's disease, cerebral ischemia and stroke (1-5).

Radical-mediated peroxidative reactions of unsaturated lipids leads to the generation of the reactive alkoxyl radical, which upon spontaneous radical elimination (β-scission) generates several saturated and unsaturated aldehydes. With ω-6 polyunsaturated fatty acids (arachidonate, linolenate, linoleate), the most abundant aldehydes generated are the 4-hydroxyalkenals. Of the various hydroxyalkenals, 4-hydroxy, trans-2-enal (HNE), generated mainly from ω-6 polyunsaturated fatty acids such as arachidonic and linoleic acids, has received considerable attention due to its high bioactivity. The electrophilic nature of α, β unsaturation in HNE renders it highly reactive with cellular nucleophiles such as glutathione, cysteine, lysine, and histidine of proteins, and with nucleic acids. HNE is generated in high concentrations during lipid oxidation and accounts for upto 95% of the total enals generated during lipid peroxidation. High concentrations of HNE are cytotoxic, whereas lower concentrations of HNE modulate cell proliferation and gene expression and cell signaling (1, 2,3, 6, 7).

Because these aldehydes are highly reactive and are generated in high concentrations, it has been suggested that they mediate and amplify the cellular effects of their radical precursors. Significant quantities of these aldehydes may also be formed by other metabolic processes such as myeloperoxidase-catalyzed oxidation of amino acids, oxidative modification of nucleosides and polyamine metabolism. Furthermore, α, β-unsaturated aldehydes are produced during metabolism of several drugs, toxicants and foods, and are ubiquitous components of pollutants(1,2,3,6,7).

Accumulation of unsaturated aldehydes or their products has been observed under several pathological conditions, e.g. proteins modified by these aldehydes have been immunochemically localized to lesions and neurons of patients with Alzheimer's(8) and Parkinson diseases (9). The tissue content of HNE is elevated approximately 3-fold over controls in diseased regions of brain and cerebrospinal fluid of patients with AD and in patients with mild cognitive impairment (6). Multiple studies show that, in diseased tissue derived from patients with AD, HNE alkylates many proteins (creatine kinase, tau, neurofilament proteins, and the glutamate transporter) whose dysfunction have neurotoxic consequences. In the cerebral cortex of patients with AD and dementia with Lewy bodies, neurons and astrocytes are immunopositive for the presence of HNE-proteins adducts (10,11,12). In Creutzfeldt-Jacob disease, the highest accumulation of HNE is in astrocytes, but not in neurons and microglial cells (5,13,14).

While high concentrations of HNE illicit toxic responses, low levels of HNE and structurally related aldehydes are involved in cell signaling. HNE exposure modulates intracellular signaling by

activating the MAPK, stress-activated protein kinase and c-Jun N-terminal protein kinase cascades (15,16) while inhibiting nuclear factor k-B activity (3,17,18). HNE affects cell surface receptor function. Studies have shown that HNE inhibits $G_{\alpha S}$ signaling of muscarinic and dopamine receptors but can cause activation of the epidermal growth factor receptor (19).

To assess the contribution of HNE and structurally related aldehydes to specific pathological states and redox signaling, it is essential to identify the metabolism of these aldehydes. Metabolism of HNE is well studies in liver and cardiovascular tissues, but the biochemical mechanisms for the metabolism of α, β -unsaturated aldehydes such as HNE is not well understood in the brain. In the present study, we have examined the metabolism of HNE in PC-12 cells.

Material and Methods

Cell culture: PC-12 Cells were cultured in 5% CO_2 - 95% atmosphere in high humidity at 37°C in Nutrient Mixture, F-12 Hams cell culture medium supplemented with 2.5% fetal bovine serum (FBS), 15% horse serum, 0.2% sodium bicarbonate and antibiotic cocktail from Gibco. For all the metabolism studies, passage 6-10 cells were used. Viability of the cells was measured by trypan blue dye exclusion.

Reagents and consumables: All the specified chemicals, reagents, diagnostic kits, were purchased from Sigma Chemical Company Pvt. Ltd. St. Louis, MO, USA, unless otherwise stated. Nutrient mixture F-12 Hams culture medium, antibiotics, fetal bovine serum and horse serum were purchased from Gibco BRL, USA. Culture wares and other plastic consumables used in the study were procured commercially from Nunc, USA. Milli Q water (double distilled deionized water) was used in all the experiments. HNE was purchased from Caymen Chemicals, U.S.A.

Chemical Synthesis of reagent HNE and its putative metabolites: The radio labeled [4-³H] HNE was synthesized from the dimethylacetal of HNE, which was oxidized to the 4-keto derivative using polymer-supported chromic acid as an oxidizing agent (1). The resulting ketone was further reduced to the dimethylacetal of HNE by using tritiated $NaBH_4$. The [4-³H] HNE obtained by acid hydrolysis was purified on HPLC. Structural identity of HNE was established by gas chromatography-mass spectroscopy (GC-MS).

1,4-Dihydroxy-2-nonene (DHN) was synthesized enzymatically by incubating 60 nmol of [4-³H]HNE with 300 milliunits of human placenta recombinant aldose reductase (AR) and 0.1 mM NADPH in 0.05 M potassium phosphate, pH 6.0, containing 0.4 M Li_2SO_4. The reaction was monitored by following the decrease in absorbance at 224 nm. The enzyme was removed by ultrafiltration using an Amicon Centriprep-10, and DHN in the filtrate was purified on HPLC as described above. Structural identity of DHN was established by gas chromatography-mass spectroscopy (GC-MS).

4-Hydroxy-*trans*-2-nonenoic acid (HNA) was synthesized by incubating 100 nmol of HNE (³H-HNE) with 1.0 unit of aldehyde dehydrogenase, and 1.5 mM NAD in 0.1 M potassium phosphate,

pH 7.4, at 25 °C. The reaction was monitored by following the increase in absorbance at 340 nm. The enzyme was removed by ultrafiltration and HNA in the filtrate was purified by HPLC. Structural identity of HNA was established by gas chromatography-mass spectroscopy (GC-MS).

The conjugate of reduced glutathione (GSH) with HNE (GS-HNE) was prepared by incubating 1 μmol of [4-³H]HNE (55,000 cpm/nmol) with 5 μmol of GSH in 0.1 M potassium phosphate, pH 7.0, for 1 h at room temperature. The reaction was monitored by following the consumption of HNE at 224 nm. The GS-HNE conjugate was purified by reverse phase HPLC as described below. For the synthesis of the reduced form of the glutathione-HNE conjugate (GS-DHN), 100 nmol of GS-HNE was incubated with 300 nmol of NADPH and 100 μg of aldose reductase in 0.1 M potassium phosphate, pH 6.0, for 3 h at 37°C. The reaction was monitored by following the consumption of NADPH at 340 nm. Structural identity of HNA was established by electrospray ionization-mass spectroscopy (GC-MS).

HPLC Analysis: Synthesized standards and metabolites of GS-HNE and GS-DHN were separated by HPLC using a Varian reverse phase ODS C_{18} column pre-equilibrated with 0.1% aqueous trifluoroacetic acid. The compounds were eluted using a gradient consisting of solvent A (0.1% aqueous trifluoroacetic acid) and solvent B (100% acetonitrile) at a flow rate of 1 ml/min. The gradient was established such that solvent B reached 24% in 20 min, 26% in 30 min, and was held at this value for 10 min. Furthermore, in the next 10 min solvent B reached 60%, and in an additional 5 min it reached 100% and was held at this value for 10 min.

Gas Chromatography–Mass Spectrometry (GC-MS): For GC-MS analyses of DHN and HNA, the samples were derivatized in 20 μl of acetonitrile with 20 μl of N,O-bis(trimethylsilyl)-trifluoroacetamide (BSTFA) for 1 h at 60°C. The mixture was cooled to room temperature and 2 μl aliquots were used for analysis. The GC-CI/MS analysis was performed using a HP5890/HP5973 GC/MS system (Hewlett Packard; Palo Alto, CA, USA) under 70 eV electron ionization conditions. The compounds were separated on a bonded phase capillary column (DB-5MS, 30 m × 0.25 mm ID × 0.25μm film thickness from J7W Scientific Folsom, CA, USA. The GC injection port and interface temperature were set to 280°C, with helium gas (carrier) maintained at 14 psi. Injections were made in the split less mode with the inlet port purged for 1 min following injection. The GC oven temperature was held initially at 100°C for 1 min and then increased at a rate of 10°C min^{-1} to 280°C, which was held for 5 min. Under these conditions, the retention time for DHN and HNA derivatives was 8.08 and 9.52 min respectively (1,2,20).

For the GC-MS analysis of HNE, 0.4 ml of a 0.05 M solution of O-(2,3,4,5,6-pentafluorobenzyl) hydroxylamine hydrochloride (PFBHA) was added to the samples and the mixtures were vortexed for 1 min and incubated for 30 min at room temperature. After incubation the samples were extracted in 4 ml hexane containing (12 drops of concentrated sulfuric acid. The mixtures were centrifuged at 2000 rpm and the upper hexane layer was aspirated and dried under nitrogen. The dried samples were

derivatized with BSTFA as described above and analyzed by GC-MS (17,21).

Electrospray Ionization Mass Spectrometry: Chemical identities of the GS-HNE and GS-DHN were established by electrospray ionization mass spectrometry (ESI/MS). The samples were analyzed on a single quadrapole Micromass LCZ instrument as described (20). The ESI+/MS operating parameters were as follows: capillary voltage, 3.0 kV; cone voltage, 13 V; extractor voltage, 9 V; source block temperature, 100 °C; and dissolvation temperature, 200 °C. Nitrogen at 3 p.s.i. was used as nebulizer gas. Samples were reconstituted in 50 μl of acetonitrile/water/acetic acid (50/50/0.1) (v/v/v), and applied to the mass spectrophotometer using a Harvard syringe pump at a rate of 5 μl/min. Spectra were acquired at the rate of 200 atomic mass units/s over the range of 20 –2000 atomic mass units.

Metabolic studies: Initial experiments described the time course of HNE metabolism. PC-12 Cells cultured in 10 cm dish were incubated in pre-warmed (37°C) modified Hank's Balanced Salt Solution (HBSS). Pre-warmed (37°C) HBSS had no observable effect on the viability of PC12 cells for the duration of the experiment. The incubation was started with the addition of 1-20 μM [³H]-HNE in 2.5 ml HBSS. Aliquots were withdrawn at indicated times, centrifuged at 10 000×g for 10 min at 4°C, and the supernatant was ultra filtered and applied to Varian ODS C_{18} reverse-phase column. The metabolites of [³H]-HNE were determined by quantifying the radioactivity in each fraction. Individual peaks were analyzed by ESI/MS or GC–CI/MS.

Inhibition of oxidoreductases: PC-12 cells were incubated in 2.5 ml HBSS without or with 0.05 mM sorbinil, 0.01 mM tolrestat, 0.5 mM miconazole or 5.0 μM benomyl for 30 min at 37°C. (³H)-HNE, 5 μM was then added in the incubation media of each sample and the incubation was carried out for an additional 30 min at 37°C. After the incubation, cells were separated from the incubation medium and the radio labeled metabolites extruded in the medium were resolved by reverse phase HPLC and analyzed by ESI/MS or GC/MS as described above.

Results

HPLC method for quantification and characterization of HNE and its metabolites: In order to characterize and quantify radio labeled HNE and its putative metabolites, we established a reverse phase HPLC method as described in *Materials and Methods.* As shown in Figure 1, HNE and most of its putative metabolites nicely separated under our chromatographic conditions. However, glutathionyl conjugates of HNE (GS-HNE) and its reduced product (GS-DHN) co-eluted with the retention time of 23 min. DHN, the reduced metabolite of HNE eluted with the retention time of 31 min, whereas HNA, the oxidized metabolite of HNE eluted with the retention time of 37 min. HNE was eluted at 43 min. For the quantification and characterization of HNE and its metabolites, one ml fractions were collected and an aliquot of each fraction (100-250 μl) was used for quantification of radioactivity whereas the remaining aliquot was used for mass spectrometric analysis as described below.
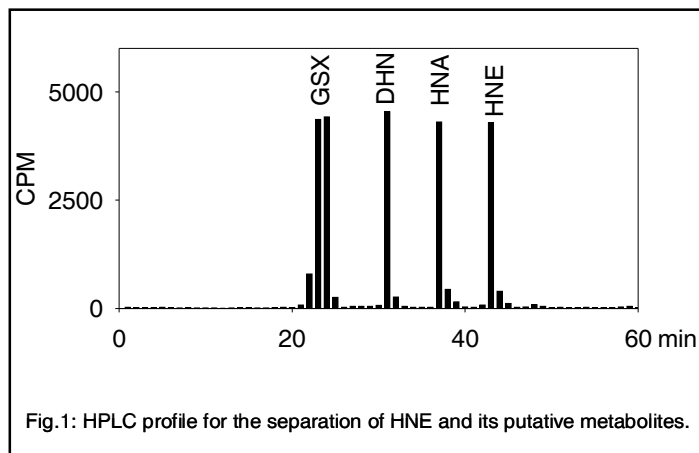

Fig.1: HPLC profile for the separation of HNE and its putative metabolites.

Characterization of glutathionyl conjugates by ESI-MS: Glutathionyl conjugate of HNE (GS-HNE) and reduced metabolite (GS-DHN) were characterized by ESI-MS. Samples corresponding to the glutathionyl conjugates (HPLC Peak I) were dried under nitrogen on speed vac and analyzed by ESI-MS as described under *Materials and Methods.* ESI-MS chromatogram of reagent GS-HNE and GS-DHN is illustrated in Fig. 2. The ESI+ mass spectrum of the reagent GS-HNE showed a molecular ion [M+H]+ with a *m/z* of 464. An additional prominent ion with *m/z* 446 was identified and ascribed to daughter ion of GS-HNE arising from the loss of a single water molecule from the parent 464 ion, because the 446 species could be completely converted at lower cone voltages to the 464 species. The ESI+ mass spectrum of reagent GS-DHN displayed a single pseudo-molecular ion [M+H]+ with a *m/z* value of 466. No daughter ions due to dehydration of the parent ion were observed.
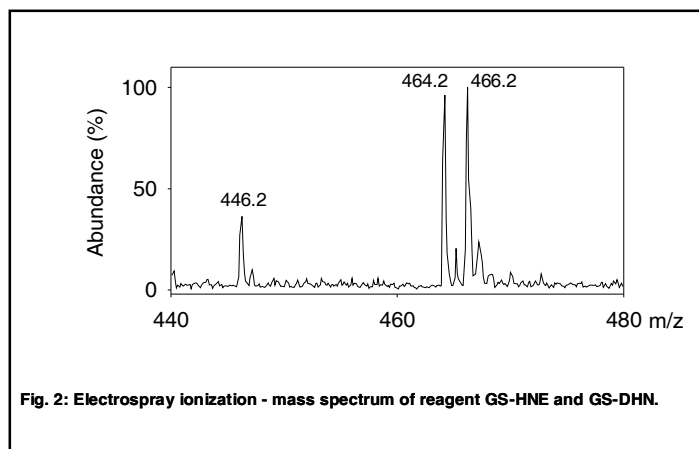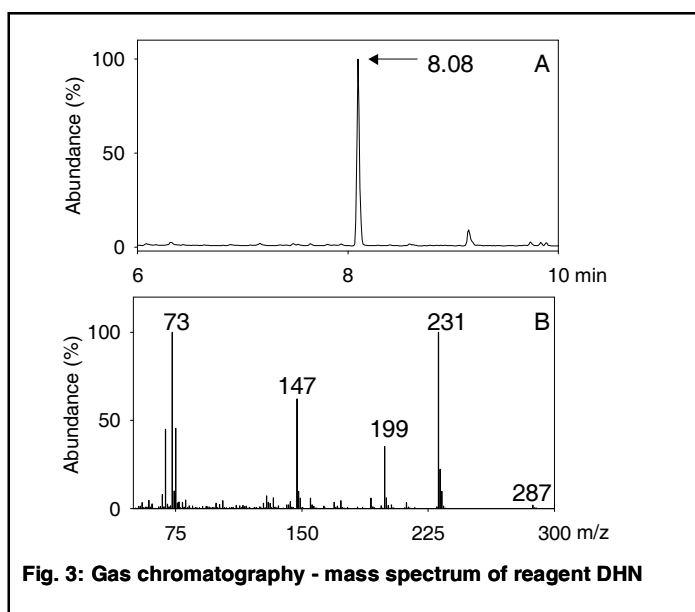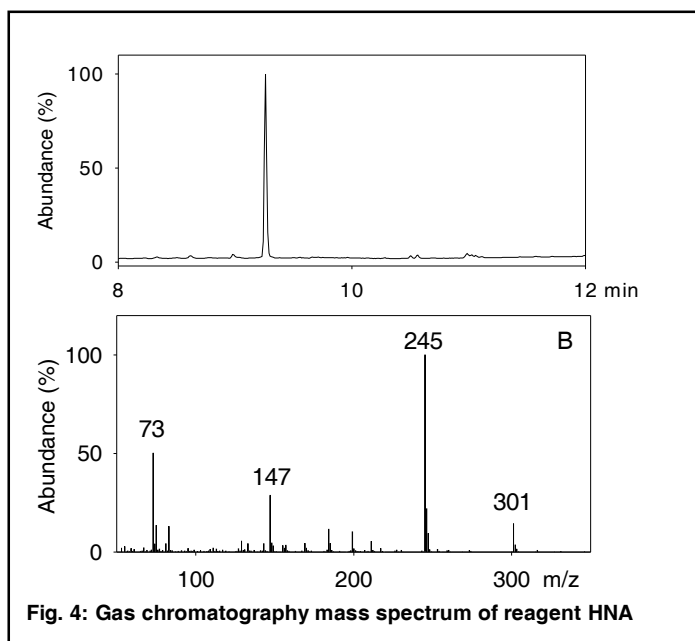

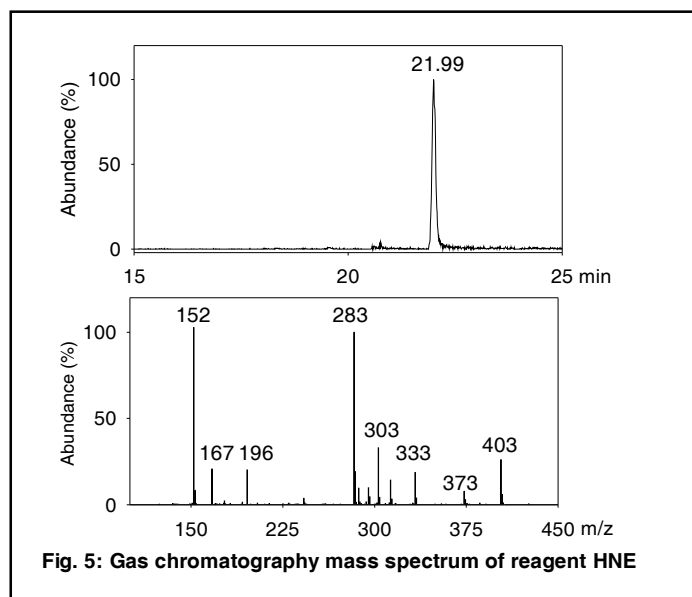Fig. 2: Electrospray ionization - mass spectrum of reagent GS-HNE and GS-DHN.

Characterization of DHN, HNA and HNE by GC-MS: For the characterization of DHN, HPLC Peak II, was subjected to GC-MS analysis. The samples were sililated as described under *Materials and Methods* and one micro liter of the derivatized sample was injected into the GC. As shown in Fig 3A, on GC, DHN eluted with the retention time of 8.08 min. Fig. 3B shows the fragmentation pattern of DHN. The signature ions with m/z values of 199, 231 and 287 were due to M-CH2OTMS (cleavage between C1-C2), M-C5H11 (saturated carbon chain where D is labeled) and M-CH3 respectively. Structural identity of HNA, HPLC Peak III, was established by GC-MS analysis. The samples

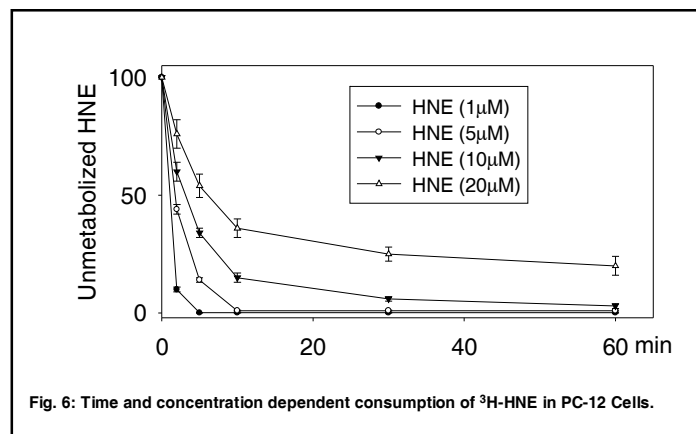Fig. 3: Gas chromatography - mass spectrum of reagent DHN

were sililated and analyzed as described for DHN. As shown in Fig 4A, on GC, HNA eluted with the retention time of 9.52 min. Fig. 4B shows the fragmentation pattern of HNA. The signature ions with m/z values of 245 and 301 were due to M-C5H11 and M-CH3 respectively. Structural identity of HNE (HPLC Peak IV) was established by GC-MS under chemical ionization conditions. Figure 5A shows the GC profile of HNE (21.99 min) and Fig. 5B shows its fragmentation pattern.

Fig. 4: Gas chromatography mass spectrum of reagent HNA

HNE consumption: To examine HNE metabolism in PC-12 cells, cells were cultured in 10cm dishes. The culture medium was removed and the cells were incubated with 1-20 μM [^{3}H]-HNE in 2.5 ml HBSS. Incubation of the cells with 1-20 μM HNE for 3 h did not cause a significant change in cell viability as determined by the MTT assay. For measuring the rate of HNE metabolism, aliquots were withdrawn at various times and the radioactivity in the medium was separated by HPLC. HNE

Fig. 5: Gas chromatography mass spectrum of reagent HNE

remaining in the medium was determined by measuring radioactivity in the peak eluting with a retention time (T_R) of the HNE. As shown in Fig. 6, PC-12cells efficiently metabolized HNE in a time and concentration dependent manner. When the cells were incubated with 1 μM [^{3}H]-HNE, ?90% of HNE was metabolized in 5 min whereas incubation of the cells with 20 μM [^{3}H]-HNE, resulted in the metabolism of $\sim$ 50% HNE in 5 min. Under these conditions, after 1h of incubation, only $\sim$ 50% unmetabolized HNE remained in the medium. The total radioactivity recovered from the incubation medium was 84±4%; =1% radioactivity was recovered from the acid-insoluble fraction after 1h of incubation.

Fig. 6: Time and concentration dependent consumption of ^{3}H-HNE in PC-12 Cells.

Quantification and characterization of HNE-derived metabolites in PC-12 cells: For the quantification and characterization of HNE-derived metabolites, PC-12 cells were incubated with 5 μM [^{3}H]-HNE for 1h. Incubation medium was separated from the cells and the radio labeled metabolites extruded in the incubation medium were separated on HPLC. Upon HPLC separation of the medium, individual peaks were assigned to specific HNE metabolites (Fig. 7) on the basis of the retention time (T_R) of synthesized standards. As shown in Fig. 7, after 1h of incubation with 5 μM [^{3}H]-HNE, 46% of the radioactivity in
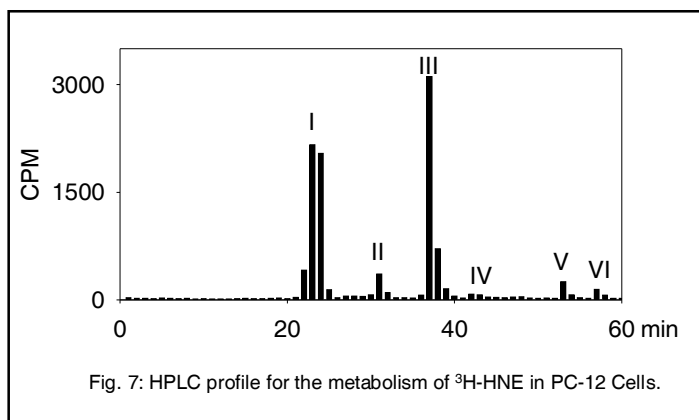
Fig. 7: HPLC profile for the metabolism of ³H-HNE in PC-12 Cells.

Fig. 9: GC-MS of DHN formed by the incubation of ³H-HNE with PC-12 Cells.

the medium was present as glutathione conjugates. Thus, conjugation with glutathione appears to be a rapid, high-affinity route of HNE elimination in PC-12 cells. Because the T_R of Peak I of the HNE-treated PC-12 cells was identical to reagent glutathionyl conjugates, fractions corresponding to this peak were subjected to ESI⁺/MS in order to characterize the metabolite(s) present in that peak. The ESI⁺ mass spectrum of HPLC Peak I showed a predominant peak at m/z 466.2, which was assigned to the +1 charge state of GS-DHN (Fig. 8). Ions with m/z values of 464.2 and 446.2 respectively, represent GS-HNE and its daughter ion originating from the in source dehydration of GS-HNE. Quantification of the signals for the ions for GS-HNE and GS-DHN showed that 62% of the conjugate was in the reduced form (GS-DHN), whereas 38 % of the conjugate was present as GS-HNE.
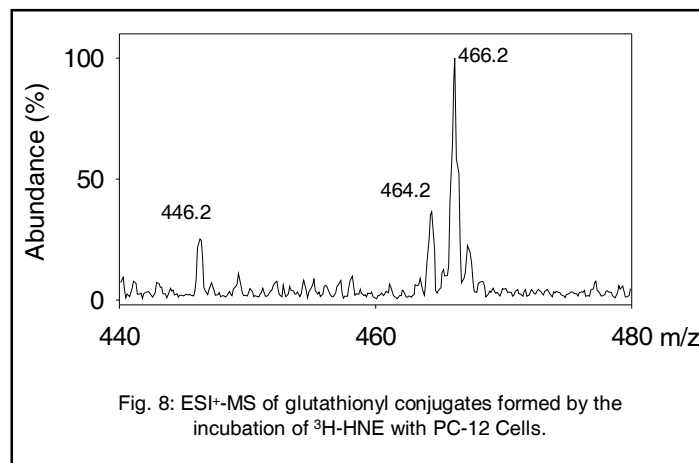

Fig. 8: ESI⁺-MS of glutathionyl conjugates formed by the incubation of ³H-HNE with PC-12 Cells.

The T_R of HPLC Peak II, which accounted for 4% of the total radioactivity, corresponded to the T_R of reagent DHN (Fig. 7). Structural identity of this peak was established by GC-MS. As shown in Fig. 9, the retention time and fragmentation pattern of this peak was identical to reagent DHN, indicating that peak II is due to DHN.

The T_R of HPLC Peak III, which represents 40% of the total radioactivity, was identical to reagent HNA (Fig. 7). To characterize this peak further, fractions corresponding to this peak were pooled, sililated and subjected to GC–CI/MS. The gas chromatograph (Fig. 10A) shows a prominent solvent-independent peak with a T_R value identical to reagent HNA. This peak was further
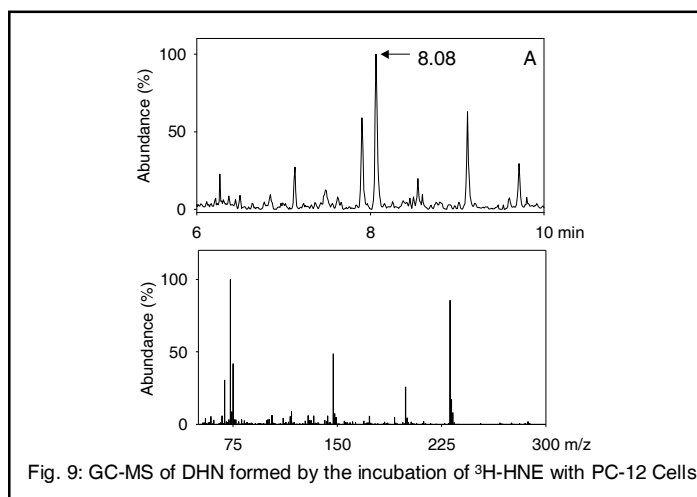
subjected to MS analysis. As shown in Fig. 10B, a molecular ion with a m/z value of 301, corresponding to derivatized HNA, was observed. The fragmentation pattern of this ion was found to be identical to that of synthetic HNA, indicating that peak III is due to HNA.
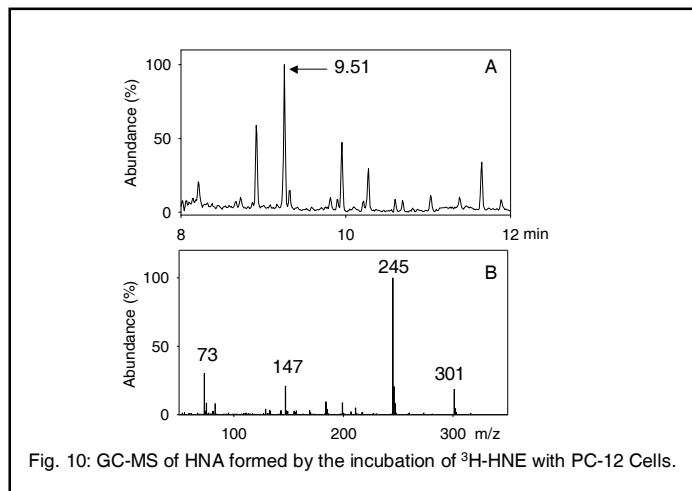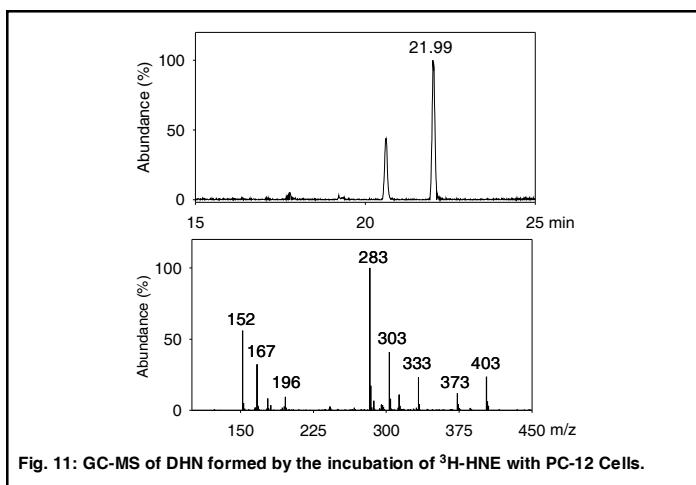

Fig. 10: GC-MS of HNA formed by the incubation of ³H-HNE with PC-12 Cells.

The HPLC, Peak IV, representing 1% radioactivity, displayed high absorbance at 224 nm and appears to be due to the unmetabolized HNE, since it eluted with a T_R value identical to reagent HNE (43 min). GC-CIMS of this peak (Fig. 11) showed that the retention time and fragmentation pattern of this peak is identical to reagent HNE, suggesting this peak is due to HNE.
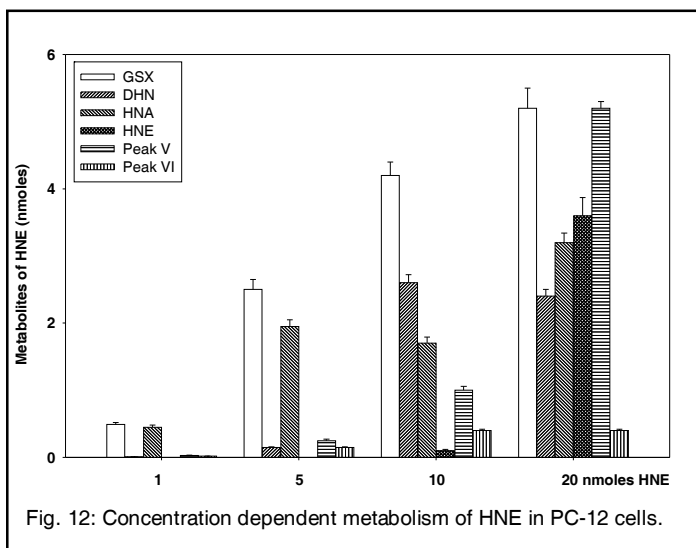
Two other peaks were observed on HPLC, eluting with the retention time of 53 (Peak V) and 57 min (Peak VI) respectively. These peaks represented 5 and 4 % radioactivity. Structural identity of these peaks has yet not been established.

Concentration dependent metabolism of HNE in PC-12 Cells: Next we examined concentration dependent metabolism of HNE in PC12 cells. As described above when PC-12 cells were incubated with 1 or 5 μM [³H]-HNE for 1h, ~ HNE was metabolized and glutathionyl conjugates and HNA were the major metabolites accounting for 90% of the metabolism. Incubation of the cells with 10 ìM [³H]-HNE for 1h, resulted in a concentration dependent increase in glutathione conjugates formation whereas

Fig. 11: GC-MS of DHN formed by the incubation of ^{3}H-HNE with PC-12 Cells.
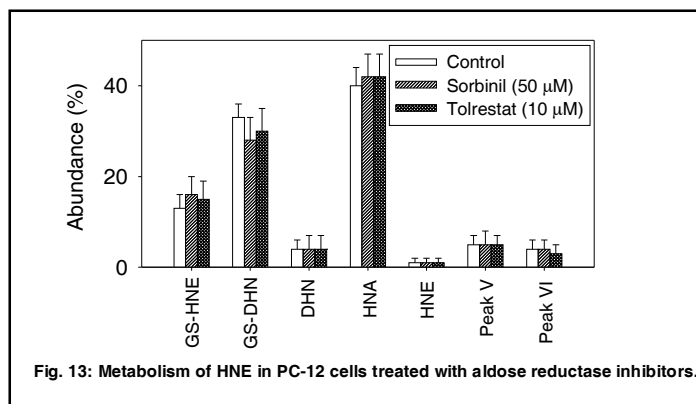
no further increase was observed in the oxidation of HNE to HNA (Fig. 12). Under these conditions, a robust increase was observed in the reduction of HNE to DHN (Fig. 12). More significant increases were also observed in the conversion of HNE to Peak V and Peak VI. Incubation of the cells with 20 μM [^{3}H]-HNE for 1h did not cause a significant change in the formation of glutathione conjugates, DHN, HNA and Peak V. However metabolism of HNE to Peak V was increased by three fold under these conditions. Moreover, 25% of HNE remained non metabolized under these conditions.
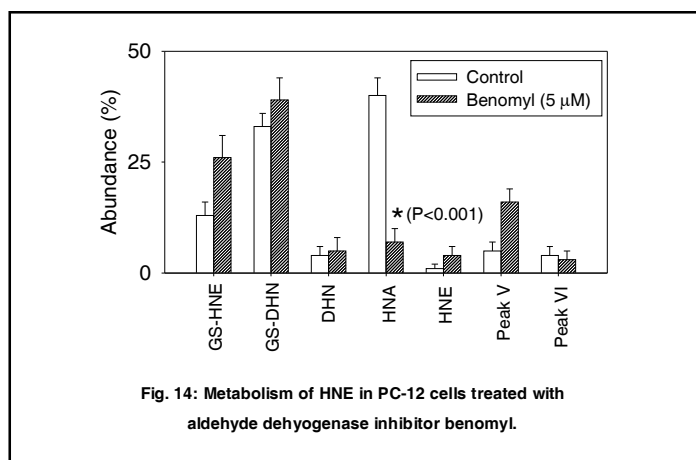

Fig. 12: Concentration dependent metabolism of HNE in PC-12 cells.

Identification of the metabolic pathways for the metabolism of HNE in PC-12 Cells: The HPLC and mass spectroscopic analyses already described clearly demonstrate that the major metabolic products of low concentrations of HNE in PC-12 cells are GS-HNE, GS-DHN and HNA. To identify the biochemical pathways involved in the formation of these metabolites, the PC-12 cells were incubated for 1 h at 37°C with inhibitors of AR (sorbinil, 50 μM or tolrestat, 10 μM), ALDH (benomyl, 5 μM) and Cytochrome P45 (miconazole 500 μM) in 2.5 ml HBSS, after which 5 ìM [^{3}H]-HNE was added to the medium, and the incubation was continued for an additional 30 min. Cells incubated with HBSS under identical conditions served as control. Incubation of the PC-12 cells with 5.0 μM HNE, with

or without these inhibitors for 3 h, did not significantly affect cell viability as determined by the MTT assay.
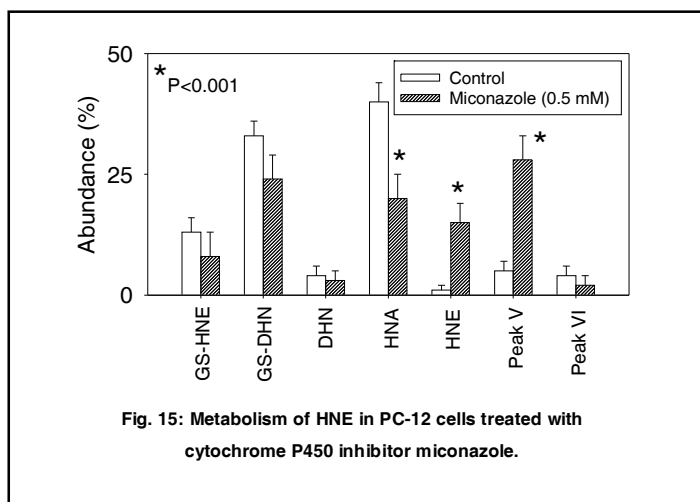
Radioactivity in the incubation medium of sorbinil or tolrestat - treated PC-12 cells separated on HPLC as described above. No change was observed in the amount of radioactivity recovered in Peaks I-VI. The ESI$^+$ mass spectrum of peak I obtained from sorbinil or tolrestat -treated cells also did not show an difference in the abundance ration of GS-HNE:GS-DHN (Fig. 13).

Fig. 13: Metabolism of HNE in PC-12 cells treated with aldose reductase inhibitors.

The metabolism of HNE in PC-12 cells was, however, significantly inhibited by the ALDH inhibitor, benomyl. (Fig. 14) The radioactivity in Peak III corresponding to HNA decreased by >75% in cells pre-incubated with benomyl as compared with those treated with [^{3}H]-HNE alone. In addition, the abundance of GS-HNE and Peak V was significantly increased in benomyl treated samples as compared to controls. Based on these observations, we infer that the formation of HNA is catalyzed by ALDH, and that inhibition of HNA formation leads to a corresponding increase in the glutathione-linked metabolism and abundance of Peak V.

Fig. 14: Metabolism of HNE in PC-12 cells treated with aldehyde dehyogenase inhibitor benomyl.

Incubation of PC-12 cells with miconazole, decreased the rate of HNE metabolism. As shown in Fig. 15 there was a >6 fold increase in the abundance of unmetabolized HNE. Miconazole also slightly inhibited the glutathionyl conjugates formation. A significant decrease (>40 %) was evident in the formation of HNA in miconazole-treated cells as compared to control. A corresponding increase was also observed in Peak V formation in maconazole-treated cells.

Fig. 15: Metabolism of HNE in PC-12 cells treated with cytochrome P450 inhibitor miconazole.

Discussion

The development of oxidative stress, in which production of highly reactive oxygen species (ROS) overwhelms antioxidant defenses, is a feature of many neurological diseases: ischemic, inflammatory, metabolic and degenerative. Oxidative stress is increasingly implicated in a number of neurodegenerative disorders characterized by abnormal filament accumulation or deposition of abnormal forms of specific proteins in affected neurons, like Alzheimer's disease (AD), Pick's disease, Lewy bodies related diseases, amyotrophic lateral sclerosis (ALS), and Huntington disease (5,10-14).

The effects of oxidative stress on "post-mitotic cells", such as neurons may be cumulative, hence, it is often unclear whether oxidative damage is a cause or consequence of neurodegeneration. Peroxidation of cellular membrane lipids, or circulating lipoprotein molecules generates highly reactive aldehydes among which one of most important is 4-hydroxynonenal (HNE). The presence of HNE is increased in brain tissue and cerebrospinal fluid of AD patients, and in spinal cord of ALS patients. Immunohistochemical studies show presence of HNE in neurofibrilary tangles and in senile plaques in AD, in the cytoplasm of the residual motor neurons in sporadic ALS, in Lewy bodies in neocortical and brain stem neurons in Parkinson's disease (PD) and in diffuse Lewy bodies disease (DLBD). Thus, increased levels of HNE in neurodegenerative disorders and immunohistochemical distribution of HNE in brain tissue indicate pathophysiological role of oxidative stress in these diseases, and especially HNE in formation of abnormal filament deposits.

Most of the studies thus far have only established that lipid derived aldehydes such as HNE, MDA and acrolein are associated with neurological disorders. However, little is known about whether HNE is casually involved in the pathogenesis of the disease process. The toxicological/pathological effect of these aldehydes would be dependent on their resident time in the cells. We have therefore examined the metabolism of HNE in PC-12 cells. Identification of the biological pathways which are involved in aldehyde metabolism would unable us to further investigate whether inhibition or over-expression of aldehyde metabolizing enzymes would alter their pathological and toxicological affects.

HNE was used as a model α,β -unsaturated aldehyde since it represents upto 95% of the total unsaturated aldehydes produced during in lipid oxidation (Esterbauer, et al., 1991). During oxidation of arachidonic acid for example, HNE is generated in 100-fold excess over malonaldehyde and glyoxal. Since it is a potent electrophile, HNE is one of the most toxic aldehydes generated during lipid peroxidation. It combines spontaneously with glutathione, and with cysteine, histidine and lysine residues of proteins, and displays a variety of cytotoxic and genotoxic effects (3).

The results of our study show that several enzymatic pathways contribute to the metabolism of HNE in neuronal cells. A distinctive feature of HNE metabolism in PC-12 cells was that most of the HNE was rapidly transformed and extruded into the incubation medium. Only a small percent (<1 %) of the radioactivity was retained by the cells. These data suggest that endogenous aldehydes generated by lipid peroxidation or other metabolic processes also may be metabolized similarly and extruded from the neuronal cells.

One of the major pathways of HNE metabolism in PC12 cells appears to be oxidation to HNA. In the liver, heart and vascular cells, HNA is generated by aldehyde dehydrogenase-catalyzed oxidation of HNE (1,2,22-24), and a similar enzymatic pathway may be responsible for HNA formation in neuronal cells. The brain contains several aldehyde dehydrogenases, including the mitochondrial aldehyde dehydrogenase, which may be responsible for catalyzing HNE oxidation. This view is strengthened by the observation that in the presence of the mitochondrial aldehyde dehydrogenase inhibitor benomyl, the formation of HNA was significantly attenuated. In addition of the mitochondrial aldehyde degydrogenase(s), results originating from Dr. Picklo's laboratory (6,10,25) also show that in the brain enals can also be oxidized by succinic semialdehyde degydrogenase (aldehyde dehyrogenase V). Further studies are required to examine the contribution of specific isozymes of aldehyde dehydrogenases in the metabolism of HNE and structurally related aldehydes in neuronal cells. Oxidation of HNE has also been suggested to be catalyzed by cytochrome P450s (26). Our data shows that inhibition of cytochrome P450s with miconazole, a non-selective P45 inhibitor, not only partially inhibited the oxidation of HNE, but also decreased the glutathiolation of HNE and slowed down HNE metabolizing capacity of the cells. IT is yet not clear whether this is a drug specific response or indeed P450 inhibitors slow down the aldehyde metabolizing ability of the cells, in which case inhibition of P450 would be deleterious rather than advantageous.

Similar to other metabolites, HNA was also rapidly extruded from the cells. Although additional investigations will be required to identify the specific transporter(s) involved in this process, it is likely that the efflux of HNA (a long chain fatty acid analog) may be mediated in part by the fatty acid transporter, which interestingly, is up-regulated during oxidative stress.

In addition to oxidation, conjugation with glutathione (GSH) also appears to be a major route of HNE metabolism in PC12 cells. We found that in these cells >45% of the metabolized HNE was in the form of GSH conjugates. The extent to which HNE is conjugated with GSH in these cells is comparable to that observed in liver (22-24), heart (1) and vascular cells (2). While HNE spontaneously reacts with GSH to form a Michael adduct, it has been proposed that intracellular formation of GS-HNE is due to glutathione S-transferase-mediated catalysis, which enhances adduct formation 600 times over the spontaneous rate (27). Several glutathione S-transferases have been localized to the brain. "HNE-specific" glutathione S-transferase (4-4 in rats and 5·8 in humans), suggested to have evolved specifically to metabolize lipid peroxidation products, is also present in the brain, although the localization and the kinetic properties of the neuronal enzyme have not been well characterized.

ESI-MS of glutathionyl conjugates showed that, in addition to GS-HNE, significant amounts of the reduced form of the conjugate-GS-DHN, were also recovered in the incubation medium of PC-12 cells incubated with HNE. The amount of GS-DHN recovered from the incubation of PC-12 cells with HNE is comparable to that formed in the cardiovascular cells. The reduced conjugate, GS-DHN, could arise either from catalytic reduction of GS-HNE or conjugation of DHN with GSH. However, due to loss of the conjugated aldehyde following reduction, it is unlikely that DHN could spontaneously react with GSH, and for the same reason, enzymatic catalysis of the adduct formation between GSH and DHN may also be inefficient. Thus, it appears unlikely that GS-DHN arises from the formation of adduct between DHN and GSH. This view is further supported by our observation that incubation of PC-12 cells with [^{3}H]DHN did not result in the formation of GS-DHN (data not shown). Thus, the most likely route of GS-DHN formation appears to be enzyme-catalyzed reduction of GS-HNE. This reductive transformation in the heart and in vascular cells is catalyzed by the polyol pathway enzyme AR. However, our observations show that in PC-12 cells, formation of GS-DHN is not catalyzed by aldose reductase since pre-incubation of PC-12 cells with aldose reductase inhibitors sorbinl and tolrestat did not inhibit GS-DHN formation. Further studies are required to investigate the biochemical pathways involved in the formation of GS-DHN in neuronal cells. Moreover, although a large fraction of the conjugate was recovered in the reduced form, the metabolic significance of this reductive transformation remains to be established. No GS-HNA adducts were recovered from PC-12 cells treated with HNE. However, mercapturic acids of HNA and its lactone cysteine have been recovered from the urine of HNE-treated rats (3,28), but these could arise from oxidation of Cys-Gly-HNE and N-acetyl-Cys-HNE rather than GS-HNE. Our data do not distinguish between these possibilities, but nevertheless, indicate that, at least in these cells oxidation of GS-HNE (in contrast to free HNE) is not catalyzed by an aldehyde dehydrogenase, and that the conjugation of HNA with GSH does not efficiently compete with HNA.

Our data also show that incubation of PC-12 cells with higher concentrations of HNE as would be expected under pathological conditions associated with enhanced oxidative stress, resulted in the increased formation of new metabolites (Peak V and VI). Although, structural identities of these compounds have not been established, Peak V co-elutes with reagent HNA-lactone. This could be an important route for the elimination of HNE when the GSTs and oxido-reductase metabolizing capacity is exhausted, particularly under the conditions of acute and severe oxidative stress.

References

1. Srivastava S, Chandra A, Ansari NH, et al. Identification of cardiacoxidoreductases involved in the metabolism of the lipid peroxidation derived aldehyde, 4-hydroxynonenal. Biochem. J 1998; 329: 469-475.

2. Srivastava S, Conklin DJ, Liu SQ, et al. Identification of biochemical pathways for the metabolism of oxidized low-density lipoprotein-derived aldehyde- 4- hydroxy trans-2-nonenal in vascular smooth muscle cells. Atherosclerosis 2001; 158 :339-350.

3. Ramana KV, Bhatnagar A, Srivastava S, et al. Mitogenic responses of vascular smooth muscle cells to lipid peroxidation-derived aldehyde 4-hydroxytrans- 2-nonenal (4-HNE): role of aldose reductase-catalyzed reduction of the 4-HNE-glutathione conjugates in regulating cell growth. J. Biol. Chem 2006; 281:17652–17660.

4. Liu X, Lovell MA, Lynn BC. Detection and Quantification of Endogenous Cyclic DNA Adducts Derived from trans-4-Hydroxy-2-nonenal in Human Brain Tissue by Isotope Dilution Capillary Liquid Chromatography Nanoelectrospray Tandem Mass Spectrometry. Chem. Res. Toxicol 2006; 19: 710-718.

5. Kubatova A, Murphy TC, Combs C, Picklo MJ. Sr. Astrocytic Biotransformation of trans-4-Hydroxy-2-nonenal Is Dose-Dependent. Chem. Res. Toxicol 2006; 19: 844-851.

6. Srivastava S, Chandra A, Wang L, etal. Metabolism of lipid peroxidation product, 4-hydroxy trans-2-nonenal in isolated rat heart. J. Biol. Chem 1998; 273: 10893-10890.

7. Srivastava S, Watowich S, Petrash JM. Structural and kinetic properties of aldehyde reduction by aldose reductase. Biochemistry 1999; 38 :42-54.

8. Sayre LM, Zelasko DA, Harris PL, etal. A. 4-Hydroxynonenal-derived advanced lipid peroxidation end products are increased in Alzheimer's disease. J Neurochem 1997; 68:2092–2097.

9. Yoritaka A, Hattori N, Uchida K. Immunohistochemical detection of 4-hydroxynonenal protein adducts in Parkinson disease. Proc Natl Acad Sci USA 1996; 93:2696–701.

10. Honzatkoa A, Brichaca J, Murphya TC. Enantioselective metabolism of trans-4-hydroxy-2-nonenal by brain mitochondria. Free Rad. Biol. & Med 2005; 39: 913 – 924.

11. Peter VU, Narasimham LP, Viswanathan N. Redox Regulation of 4-Hydroxy-2-nonenal-mediated Endothelial Barrier Dysfunction by Focal Adhesion, Adherens, and Tight Junction Proteins*. J. Biol. Chem 2006; 281: 35554–35566.

12. Oyamada R, Hayashi M, Katoh Y, etal. Neurofibrillary tangles and deposition of oxidative products in the brain in cases of myotonic dystrophy. Neuropathology 2006; 26: 107–114.

13. Leea E.J, Chenab HY, Leea MA, etal. Cinnamophilin reduces oxidative damage and protects against transient focal cerebral ischemia in mice. Free Rad Biol & Med 2005; 39:495 – 510.

14. Williams TI, Lynn BC, Markesbery WR, Lovell MA. Increased levels of 4-hydroxynonenal and acrolein, neurotoxic markers of lipid peroxidation, in the brain in Mild Cognitive Impairment and early Alzheimer's disease. Neurobiol. of Aging 2006; 27: 1094–1099.

15. Abdul HM, Butterfield DA. Involvement of PI3K/PKG/ERK1/2 signaling pathways in cortical neurons to trigger protection by co-treatment of acetyl-L-carnitine and alpha-lipoic acid against HNE-mediated oxidative stress and neurotoxicity: implications for Alzheimer's disease. Free Radic Biol Med 2007; 42: 371-384.

16. Sharma R, Sharma A, Dwivedi S, Zimniak P, et al. 4-Hydroxynonenal self-limits fas-mediated DISC-independent apoptosis by promoting export of Daxx from the nucleus to the cytosol and its binding to Fas. Biochemistry 2008; 47:143-156.

17. Srivastava S, Chandrasekar B, Bhatnagar A, Prabhu S. Lipid peroxidation derived aldehydes and oxidative stress in the failing heart: role of aldose reductase. Am. J. Physiol 2002; 283 :H2612-H2619.

18. Srivastava S, Ramana KV, Tammali R, et al. Contribution of aldose reductase to diabetic hyperproliferation of vascular smooth muscle cells. Diabetes 2006; 55:901-910.

19. Jenner P. Oxidative stress in Parkinson's disease. Ann Neurol 2003; 53: S26-36.

20. Srivastava S, Dixit BL, Cai J, et al. Metabolism of lipid peroxidation product, 4-hydroxynonenal (HNE) in rat erythrocytes: Role of aldose reductase. Free Radic Biol Med 2000; 29: 642-651.

21. Shinmura K, Bolli R, Tang XL, et al. Aldose reductase is an obligatory mediator of the late phase of ischemic preconditioning. Circ. Res 2002; 91:240-246.

22. Hartley DP, Kroll DJ, Petersen DR. Prooxidant-initiated lipid peroxidation in isolated rat hepatocytes: detection of 4-hydroxynonenal- and malondialdehyde-protein adducts. Chem Res Toxicol 1997; 10: 895-905.

23. Sampey BP, Stewart BJ, Petersen DR. Ethanol-induced modulation of hepatocellular extracellular signal-regulated kina.se-1/2 activity via 4-hydroxynonenal. J Biol Chem 2007; 282:1925-37.

24. Stewart BJ, Doorn JA, Petersen DR. Residue-specific adduction of tubulin by 4-hydroxynonenal and 4-oxononenal causes cross-linking and inhibits polymerization. Chem Res Toxicol 2007; 8:1111-1119.

25. Melissa J.M, Darryl EM, Venkataraman A, MJ Picklo. Sr. Metabolism of 4-Hydroxy-*trans*-2-nonenal by Central Nervous System Mitochondria Is Dependent on Age and NAD+ Availability. Chem. Res. Toxicol 2004; 17: 1272-1279.

26. Amunom I, Stephens LJ, Tanasi V, et al. Cytochromes P450 catalyze oxidation of á,â-unsaturated aldehydes. Arch. Biochem. Biophy 2007; 464: 187-196.

27. Awasthi YC, Yang Y, Tiwari NK, et al. Regulation of 4-hydroxynonenal-mediated signaling by glutathione S-transferases. Free Radic Biol Med 2004; 37: 607-619.

28. Alary J, Fernandez Y, Debrauwer L, et al. Identification of intermediate pathways of 4-hydroxynonenal metabolism in the rat. Chem Res Toxicol 2003; 16 :320-7.